

Carbon-13 NMR Relaxation Study of the Internal Dynamics in Cyclodextrins in Isotropic Solution

Piotr Bernatowicz,^{*,†} Katarzyna Ruszczyńska-Bartnik,[‡] Andrzej Ejchart,[‡] Helena Dodziuk,[†] Ewa Kaczorowska,[‡] and Haruhisa Ueda[§]

Institute of Physical Chemistry, Polish Academy of Sciences, Kasprzaka 44/52, 01-224 Warsaw, Poland, Institute of Biochemistry and Biophysics, Pawińskiego 5a, 02-106 Warsaw, Poland, and Department of Physical Chemistry, Hoshi University, 4-41 Ebara 2-chome, Shinagawa-ku, Tokyo 142-8501, Japan

Received: September 2, 2009; Revised Manuscript Received: November 5, 2009

¹³C nuclear spin relaxation processes in seven cyclodextrins (from six-membered α to twelve-membered η) were investigated in ²H₂O solution at multiple magnetic fields. Detailed analysis of ¹³C longitudinal relaxation in laboratory and rotating frames and ¹³C{¹H} nuclear Overhauser enhancement in these molecules yielded their rotational diffusion tensors and a semiquantitative picture of their internal dynamics.

1. Introduction

For more than 30 years macrocyclic oligosugars—cyclodextrins, CDs¹—were considered to have a rigid, truncated-cone structure.^{2,3} Such a structure of C_n symmetry ($n = 6$ for α -CD, **1**, 7 for β -CD, **2**, etc.) with all glycosidic oxygen atoms lying in a plane and forming a regular polygon stemmed from X-ray studies, although the analyses of native CD geometries ($n = 6$ – 8) using this technique did not show such a high symmetry, and only averaged parameters for their structure are given in the reviews by Harata.^{4,5} This opinion on the rigidity of native CDs contradicts model considerations, since the macrocycles are built of relatively rigid glucopyranose units connected by the glycosidic bonds characterized by a low barrier of 1 kcal/mol to internal rotation.⁶ Model molecular mechanics calculations on **1** yielded asymmetric structures corresponding to broad energy minima.⁷

Considering CDs as rigid molecules did not change even after discovery of the flip-flop mechanism interchanging the direction of the O2H and O3H hydrogen bonds in the macrocycles.⁴ On the other hand, ¹H and ¹³C NMR spectra of CDs in liquids display chemical shift equivalence of corresponding protons and carbons of glucopyranose units, pointing either to highly symmetrical structures or to the intramolecular motions fast on the chemical shift time scale.⁸ The first possibility is incompatible with the disappearance of the broad ν_{OH} band at ca. 3400 cm⁻¹ in the Raman spectra of microcrystalline β -CD \cdot 12H₂O after exposure to ²H₂O or H₂¹⁷O in view of the obstacles posed by the densely packed crystal lattice to the rapid movement of water molecules. This movement could be feasible only by structural fluctuations of the CD molecules temporarily opening appropriate diffusion paths.⁹ The crystallization of **1** (and also **2** and **3**) with different amounts of water molecules^{4,5} as well as the facility of complexation of guest molecules of various shapes¹ would not be possible without a considerable degree of CD flexibility. The nonrigidity of CD complexes and the guest mobility inside the CD cavity was in discussed in detail in refs 2 and 3. In particular, two cases of substituted CDs were

reported, for which the internal motions of the macrocycles were at least partly frozen at low temperature manifested by a considerable broadening and/or splitting of NMR signals.^{10,11}

In spite of the finally recognized CD flexibility, no experimental attempt was undertaken to provide a specific picture of their internal mobility in solution. The NMR relaxation studies performed by Kowalewski et al.,^{12,13} although originally aiming at investigations of the CD dynamics, interpreted the experimental results in terms of the Lipari–Szabo formalism.¹⁴ This approach is easy in implementation since it does not require any physical picture of the internal dynamics, yet as a result, it delivers, apart from the global correlation time, the values of generalized order parameters, S^2 , the physical meaning of which is not precisely defined, and values of effective correlation times characterizing intramolecular motions. The latter quantities absorb the discrepancies between the relaxation parameters measured and calculated on the basis of an assumed model of global molecular reorientation, so that, by definition, they do not provide insight into a real molecular dynamics. This is a serious limitation of the Lipari–Szabo analysis. The present study attempts to fill this gap. It demonstrates that nuclear spin relaxation methods supported by pertinent theoretical models do allow for efficient simultaneous investigations of both global and internal molecular dynamics.

In the present investigations, only the ¹³C relaxation rates of the ring carbon atoms, measured under conditions of proton decoupling, are exploited. The use of such a limited experimental data set is deliberate. Under the above conditions, the longitudinal relaxation behavior of the ¹³C nucleus in a CH grouping is monoexponential¹⁵ so that error-prone decomposition of the recovery curves into single-exponential components is avoided. Moreover, the observed relaxation rate is almost completely dominated by the dipolar C–H interaction within the grouping and is independent of cross-correlations with other time-dependent interactions present in the system. In this way, difficult questions about the strengths of the latter need not be addressed. It must also be stressed that the ¹H relaxation data are virtually useless for the present study. Apart from the already mentioned problems with evaluation of the relevant interaction strengths, the possible exploitation of the proton data is hampered also by the fact that in CDs the proton resonances come in partially overlapping multiplets. The individual com-

* To whom the correspondence should be addressed. E-mail: bernat@ichf.edu.pl.

[†] Polish Academy of Sciences.

[‡] Institute of Biochemistry and Biophysics.

[§] Hoshi University.

ponents of the latter can in general relax with different rates for which closed-form expressions are nonexistent. By and large, dipolar proton–proton interactions within the same glucopyranose ring do not exceed much the corresponding interactions between the neighboring rings. Thus, the network of interactions that needs to be taken into account for an adequate description of the relaxation behavior of the ring protons is too extensive even for treatment in terms of the Redfield relaxation matrix.

2. Experimental Section

α -, β -, and γ -CD (Sigma) were used without further purification. The large-ring CDs, δ - η , were obtained as described in ref 16. NMR samples of 650 μ L contained 10 mM CD solutions in $^2\text{H}_2\text{O}$ (Armar Chemicals). ^1H and ^{13}C resonance assignments of methine groups were done de novo from 2D DQF-COSY and $^1\text{H}/^{13}\text{C}$ HSQC spectra (Supporting information). All chemical shifts in heteronuclear NMR spectra were reported with respect to external DSS- d_4 . Chemical shifts of ^{13}C signals were assigned indirectly using the ratio of the zero-point frequencies, $f(^{13}\text{C})/f(^1\text{H}) = 0.251\,449\,530$.¹⁷

The ^{13}C longitudinal relaxation rates in the laboratory ($R_{1\text{C}}$) and rotating ($R_{1\rho\text{C}}$) frames and $^{13}\text{C}\{^1\text{H}\}$ nuclear Overhauser enhancements (η_{C}) were measured at magnetic fields of 11.7, 9.4, and 7.0 T, using Varian Unity Plus 500 MHz, Varian Unity Inova 400 MHz, and Bruker Avance II 300 MHz spectrometers, respectively. The temperature was set at 300.6 K in all experiments.

Both relaxation rates were determined using a series of 2D double INEPT based experiments with sensitivity enhancement adapted to ^{13}C from ^{15}N sequences.¹⁸ The original R_2 experiment was adopted to $R_{1\rho}$ measurements by substitution of the CPMG sequence with the spin-lock train of contiguous 180° pulses on ^{13}C with alternating phases.¹⁹ The amplitudes of the spin-lock field were 1.66, 1.33, and 3.84 kHz at 11.7, 9.4, and 7.0 T, respectively. The $R_{1\text{C}}$ and $R_{1\rho\text{C}}$ data were obtained using ten evolution delays within the range of 0–55 ms and seven evolution delays within the range of 5–26 ms, respectively. Appropriate ^1H 180° pulses were used during evolution of relaxation to suppress the effect of dipolar/CSA cross-correlation.²⁰ The recycle delays were always longer than 5 times the longest proton T_1 , usually exceeding 2 s. The steady-state heteronuclear $^{13}\text{C}\{^1\text{H}\}$ NOEs were determined as a ratio of cross-peak intensities in two experiments, with and without proton presaturation. The appropriate sequence was taken from ref 19 and optimized for ^{13}C . Since NOE measurements started from ^{13}C magnetization, the recycle delay had to be longer than 10 times the carbon T_1 , typically 5.1 s.²¹

Each 2D spectrum was acquired with 512 (t_2) \times 128 (t_1) complex data points with four transients per increment. Spectral widths were 1900 Hz in the ^1H dimension and 8000 Hz in the ^{13}C dimension. Zero filling was performed prior to the Fourier transformation. Data were processed using the program nmrPipe²² and analyzed with the program SPARKY.²³ Resonance intensities were used in calculating relaxation times and NOE values. All the experiments were repeated at least twice. Experimental errors of the relaxation rates were obtained from appropriate elements of the variance–covariance matrix. Experimental errors in NOE values were evaluated from the formula $\sigma_{\text{NOE}} = (1 + \eta_{\text{C}})[(S/N)_{\text{s}}^{-2} + (S/N)_{\text{ns}}^{-2}]^{1/2}$, where $(S/N)_{\text{s}}$ and $(S/N)_{\text{ns}}$ denote signal-to-noise ratios in ^1H saturated and ^1H nonsaturated spectra, respectively.²⁴ Experimental errors of NOE obtained in such a way were very close to those derived from the analysis of 10 separate measurements performed for **6** at 7.0 T.

All the spectrometers were equipped with variable-temperature units allowing for temperature control with an accuracy of 0.1 K. Temperature calibration was carefully performed using an ethylene glycol chemical shift thermometer.²⁵ Both the gas flow and decoupling power were carefully controlled²⁶ to diminish temperature gradients in the samples. Spectrometers were stabilized for at least 2 h before the beginning of the measurements.

Components of cyclodextrin rotational diffusion tensors (RDTs) were obtained from a least-squares iterative analysis of the relaxation data performed using a Fortran routine written in-house, based on the Newton–Raphson algorithm.²⁷

3. Results and Discussion

References 28 and 29 contain a formalism necessary to link the molecular dynamics, both global and local, to spectral densities, $J(\omega)$, the impact of which on NMR observables, such as the ^{13}C longitudinal relaxation rate, $R_{1\text{C}}$, ^{13}C – ^1H cross-relaxation rate, ρ_{C} , and relaxation rate in a rotating frame, $R_{1\rho\text{C}}$, is well established.^{15,30–33}

$$R_{1\text{C}} = T_{1\text{C}}^{-1} = \frac{1}{20}[J(\omega_{\text{H}} - \omega_{\text{C}}) + 3J(\omega_{\text{C}}) + 6J(\omega_{\text{H}} + \omega_{\text{C}})] \quad (1)$$

$$\rho_{\text{C}} = \frac{\eta_{\text{C}}\gamma_{\text{C}}R_{1\text{C}}}{\gamma_{\text{H}}} = \frac{1}{20}[6J(\omega_{\text{H}} + \omega_{\text{C}}) - J(\omega_{\text{H}} - \omega_{\text{C}})] \quad (2)$$

$$R_{1\rho\text{C}} = T_{1\rho\text{C}}^{-1} = \frac{1}{40}[(4 \sin^2 \xi)J(\omega_1) + (2 - \sin^2 \xi)J(\omega_{\text{H}} - \omega_{\text{C}}) + (6 - 3 \sin^2 \xi)J(\omega_{\text{C}}) + (6 \sin^2 \xi)J(\omega_{\text{H}}) + 6(2 - \sin^2 \xi)J(\omega_{\text{H}} + \omega_{\text{C}})] \quad (3)$$

In eqs 1–3 ω_{H} and ω_{C} denote ^1H and ^{13}C Larmor frequencies, respectively. ξ is defined by $\tan \xi = \omega_1/\Delta$, where ω_1 is the amplitude of the radio frequency field expressed in angular frequency units and Δ is the offset frequency for a given ^{13}C nucleus.

Since proton-decoupled ^{13}C spectra of all CDs under investigation contain in liquids only six signals manifesting high symmetry of the average NMR Hamiltonian, we assume the global motions of these molecules to be represented by axially symmetric RDTs with D_x and D_y equal and denoted by D_{\perp} while the distinct D_z component is further denoted by D_{\parallel} . As a mechanism for the local dynamics we assume diffusion of a glucopyranose unit about the axis interconnecting its glycosidic oxygen atoms, O1 and O4 (see Figure 1).

Since refs 28 and 29 do not comprise such a mechanism of the internal motion, we describe it by discrete dynamics taking place in very tiny steps. Populations of individual conformers assumed in this process are weighted by Gaussian-shaped distributions. Unfortunately, the exchange rates of interconversion of these conformers, which influence the most general eq 12 of ref 28 and eq 14.2 of ref 29, are not known. We avoid this problem by assuming that the local dynamics is either very slow or very fast in comparison to the global molecular reorientation. In such cases the spectral densities of interest are given by

$$J_{\text{slow}}(\omega) = \sum_{i=1}^N p_i D_{i,\text{CH}}^2 \sum_{r=0}^2 A_{ri}^2 \frac{2\tau_r}{1 + (\omega\tau_r)^2} \quad (4)$$

and

$$J_{\text{fast}}(\omega) = \tilde{D}_{\text{CH}}^2 \sum_{r=0}^2 \tilde{A}_r^2 \frac{2\tau_r}{1 + (\omega\tau_r)^2} \quad (5)$$

where

$$\begin{aligned} \tau_0 &= (6D_{\perp})^{-1} \\ \tau_1 &= (5D_{\perp} + D_{\parallel})^{-1} \\ \tau_2 &= (2D_{\perp} + 4D_{\parallel})^{-1} \end{aligned} \quad (6)$$

and

$$\begin{aligned} A_{0i} &= \frac{3 \cos^2 \Theta_i - 1}{2} \\ A_{1i} &= \frac{\sqrt{3}}{2} \sin 2\Theta_i \\ A_{2i} &= \frac{\sqrt{3}}{2} \sin^2 \Theta_i \end{aligned} \quad (7)$$

with N and p denoting the number of conformers and their populations, respectively. Θ is the angle between the CH vector and the z axis of the RDT, while $D_{\text{CH}} = -(\mu_0 \hbar \gamma_C \gamma_H / 4\pi) (r_{\text{CH}}^{-3})$ is the ^{13}C - ^1H dipolar coupling constant. A tilde over a symbol denotes averaging over all the conformers, i.e., $\tilde{X} = \sum_{i=1}^N p_i X_i$. The spectral densities of eqs 4 and 5 are not explicitly dependent on the exchange matrix elements. In further analysis it is assumed that the spectral densities in eqs 1–3 are dependent only on the motional behavior of a single glucopyranose unit. Therefore, the effects of instantaneous correlations of motion of the glucopyranose unit of interest with the neighboring glucopyranose units can be neglected. Due to the above-mentioned symmetry of the average NMR Hamiltonian, the

conclusions concerning a single unit are representative for all the units in a CD molecule.

In most instances relaxation of ^{13}C nuclei is realized by two main mechanisms: modulation of the dipolar interaction to the neighboring proton nuclei and modulation of their own chemical shielding anisotropies (CSAs). Since the CSA of aliphatic CH carbons of CDs is small, ca. 30–40 ppm,³⁴ we can safely neglect the latter mechanism at magnetic fields of 7.0–11.7 T. The error caused by this approximation is estimated to be not larger than about 2%. Possible interference of dipolar and CSA mechanisms has been suppressed with ^1H pulses (see the Experimental Section).

To calculate the D_{CH} values, which are needed for the description of dipolar relaxation, neutron diffraction geometries of CDs are exploited, both native^{35–38} and in complexes.^{39–41} The procedure is as follows. For each CH bond in a single glucopyranose unit its mean length was calculated. The averaging was carried out over all the units whose neutron geometries had been found in refs 35–41. Then we used the neutron geometry of an arbitrary glucopyranose unit, including both its glycosidic oxygens, but the lengths of all CH bonds were adjusted to calculated averages by shifting the proton positions along the respective CH bonds. The long-range D_{CH} values were then calculated directly from such a geometry, while one-bond D_{CH} values were further corrected; i.e., they were multiplied by so-called vibrational correction,⁴² ξ . The magnitude of this correction, which was assumed to be the same for all one-bond D_{CH} values, was fitted simultaneously with other parameters in a numerical routine. The remaining parameters adjusted to “best fit” the measured relaxation data were the components of the RDTs, D_{\parallel} and D_{\perp} , and two angles, α and β , positioning the glucopyranose unit in the RDT coordinate frame. These angles do not have absolute sense. They describe the equilibrium orientation in the RDT coordinate frame of the glucopyranose unit, determined in the iterative minimization procedure, relative to an initial, arbitrary orientation of the CD molecule concerned, specified in the program input. Precisely, the equilibrium orientation is obtained as an effect of two rotations of the glucopyranose unit, first by angle α about axis z and then by angle β around axis y of the RDT frame.

The analyzed data include both $R_{1\text{C}}$ values and ρ_{C} values. The former often have 1 order of magnitude larger values than the latter, so that the influence of both these data types on the results might not be comparable. Therefore, prior to the analysis, the individual $R_{1\text{C}}$ values and ρ_{C} values are weighted by the reciprocal of the averages of the respective quantities calculated for each CD, ensuring a similar impact on the results.

The $R_{1\rho\text{C}}$ data, although they had been acquired, were not exploited at this stage for the following reason: the ξ entering eq 3 is a function of the frequency offset, Δ , which may vary for each ^{13}C nucleus among conformers along with their chemical shifts. Since the latter quantities for individual conformers are not known, we are not able to calculate the $R_{1\rho\text{C}}$ in the slow local dynamics regime. The situation is different in the fast local dynamics regime, where eq 3 requires ξ averaged over all conformers, so that the knowledge of the individual chemical shifts for consecutive conformers is not required. Since the discrimination between fast and slow local dynamics had to be done, the $R_{1\rho\text{C}}$ values were rejected to compare identically processed data sets. Ultimately, they were calculated a posteriori (see below). For the slow local dynamics regime averaged chemical shifts were used perforce, so that the resulting values should be considered with caution.

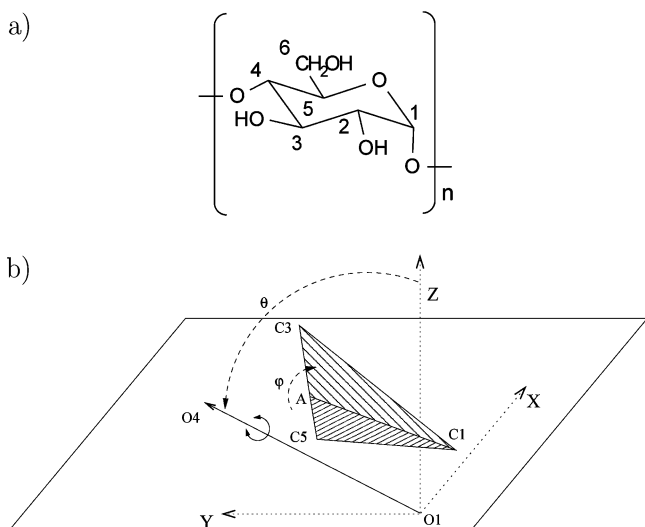


Figure 1. (a) α -, β -, ..., η -CDs, 1–7 ($n = 6$ –12, respectively), and the atom numbering in the glucopyranose unit. (b) Schematic drawing of the orientation of a single glucopyranose unit in the reference frame of the RDT of a CD molecule. The segment A–C1 is the intersection of the triangle spanned by C1, C3, and C5 atoms with the xy plane of the RDT, coplanar with the average plane of glycosidic oxygen atoms. The angle between the C1–C3–C5 plane and the xy plane of the RDT is denoted by φ . The angle between the z axis of the RDT and the O1–O4 axis is denoted by θ . The geometry of the C1–C3–C5 plane with respect to the O1–O4 axis is fixed; all these atoms are constituents of the glucopyranose unit assumed to be rigid. The double arrow depicts the internal dynamics, i.e., diffusion of the glucopyranose unit about the O1–O4 axis. Populations of the conformers arising as the result of this process are described by a Gaussian function whose width at half-height is given by the GHW parameter listed in column 1 of Table 1.

TABLE 1: Results of Numerical Iterative Analysis Which Passed the Selection Procedure Described in the Text

GHW (deg)	rmsd	D_{\perp} (10^9 s $^{-1}$)	D_{\parallel} (10^9 s $^{-1}$)	φ (deg)	θ (deg)	ζ
α -CD, Fast Internal Dynamics						
20	0.0531	0.126 ± 0.023	0.798 ± 0.144	78 ± 24	74 ± 44	0.958 ± 0.006
25	0.0526	0.120 ± 0.023	0.812 ± 0.124	76 ± 24	73 ± 39	0.965 ± 0.007
β -CD, Fast Internal Dynamics						
25	0.0550	0.100 ± 0.029	0.627 ± 0.119	72 ± 15	82 ± 9	0.956 ± 0.005
30	0.0558	0.097 ± 0.030	0.637 ± 0.122	71 ± 14	80 ± 8	0.963 ± 0.006
γ -CD, Slow Internal Dynamics						
55	0.0464	0.007 ± 0.020	0.846 ± 0.168	56 ± 8	79 ± 3	0.961 ± 0.011
δ -CD, Slow Internal Dynamics						
45	0.0538	0.001 ± 0.016	0.954 ± 0.102	51 ± 5	76 ± 2	0.962 ± 0.008
50	0.0538	0.003 ± 0.015	0.925 ± 0.121	51 ± 5	76 ± 2	0.963 ± 0.008
65	0.0519	0.007 ± 0.016	0.853 ± 0.151	53 ± 8	77 ± 3	0.965 ± 0.009
70	0.0518	0.006 ± 0.018	0.832 ± 0.163	54 ± 9	77 ± 4	0.967 ± 0.011
75	0.0531	0.002 ± 0.022	0.799 ± 0.162	57 ± 10	76 ± 5	0.970 ± 0.014
ϵ -CD, Slow Internal Dynamics						
55	0.0442	0.001 ± 0.013	0.810 ± 0.095	50 ± 5	78 ± 2	0.966 ± 0.008
60	0.0450	0.001 ± 0.015	0.789 ± 0.109	51 ± 6	77 ± 2	0.967 ± 0.009
70	0.0452	0.003 ± 0.014	0.775 ± 0.109	51 ± 6	76 ± 2	0.969 ± 0.009
75	0.0452	0.004 ± 0.014	0.770 ± 0.110	51 ± 7	76 ± 3	0.969 ± 0.010
80	0.0446	0.004 ± 0.013	0.767 ± 0.106	50 ± 7	77 ± 3	0.970 ± 0.010
ζ -CD, Slow Internal Dynamics						
80	0.0555	0.002 ± 0.017	0.742 ± 0.122	50 ± 8	77 ± 3	0.968 ± 0.013
85	0.0567	0.002 ± 0.018	0.741 ± 0.131	50 ± 9	76 ± 4	0.968 ± 0.014
90	0.0557	0.002 ± 0.018	0.739 ± 0.122	49 ± 9	77 ± 4	0.969 ± 0.014
η -CD, Slow Internal Dynamics						
65	0.0709	0.003 ± 0.019	0.692 ± 0.122	48 ± 8	78 ± 3	0.964 ± 0.015
75	0.0741	0.006 ± 0.021	0.688 ± 0.138	48 ± 9	76 ± 4	0.964 ± 0.016
80	0.0717	0.006 ± 0.019	0.683 ± 0.125	47 ± 9	77 ± 3	0.965 ± 0.015
90	0.0720	0.006 ± 0.020	0.681 ± 0.128	46 ± 11	77 ± 4	0.965 ± 0.017

287 The iterative analyses were performed for each CD, under
 288 assumptions of both slow and fast internal dynamics. The latter
 289 is represented by the set of conformers, weighted by Gaussian-
 290 shaped distributions, arising as a result of rotation of the
 291 glucopyranose unit about the axis connecting its terminal
 292 glycosidic oxygens. The widths at half-height of the Gaussian
 293 distributions, GHW, are varied from 5° to 90° with steps of 5° .
 294 This procedure yielded 36 preliminary results per CD.

295 Part of these results were rejected on the basis of the following
 296 criteria: (i) sets with negative RDT components, (ii) sets whose
 297 rmsd was higher by 5% or more in comparison to the best rmsd
 298 for a given CD, (iii) sets with vibrational correction higher than
 299 0.97, (iv) sets where the angle between the axis connecting
 300 glycosidic oxygens and the z axis of the RDT, θ , is smaller
 301 than 60° . The limit of 0.97 in point iii was chosen somewhat
 302 arbitrarily. The vibrational correction of the one-bond CH
 303 dipolar coupling constant should be between 0.83 and 0.95.^{42–46}
 304 We are aware of the fact, however, that the present analysis
 305 neglects relaxation arising from sources other than modulation
 306 of the intramolecular $^{13}\text{C}-^1\text{H}$ dipolar interactions. It is also not
 307 able to account for relaxation caused by the internal dynamics,
 308 if it happens that, contrary to the assumptions, the rates of the
 309 latter processes are comparable to the magnitudes of the RDT
 310 components. For these reasons vibrational corrections higher
 311 than those mentioned in refs 42–46 might be expected. On the
 312 other hand, ref 42 quotes the value of 0.97 as a vibrational
 313 correction caused by stretching vibrations, and being indepen-
 314 dent of the temperature, environment, and molecular structure.
 315 Therefore, this value seems to be a reasonable choice for its
 316 upper limit. The value of 60° in condition iv is also somewhat
 317 arbitrary. Mentioned angles lower than a certain value lead to
 318 close van der Waals contacts of atoms belonging to neighboring
 319 glucopyranose units, but due to the vague definition of the van

der Waals radii there is no justification for any specific value
 of this angle.

Sets of the results of numerical analyses, which passed the
 described selection procedure, are listed in Table 1. The RDT
 components and angles θ and φ are also visualized in Figures
 2 and Figure 3, respectively.

The consecutive columns of Table 1 contain the widths at
 half-height of Gaussian distributions weighting individual
 conformers about the O1–O4 axis (GHW), the rmsd of each
 iterative analysis, the D_{\perp} and D_{\parallel} components of the RDTs, the
 tilt of the glucopyranose plane (defined by carbon atoms 1, 3,
 and 5) with respect to the xy plane of CD (φ), the angle between
 the z axis of the cyclodextrin RDT and the O1–O4 axis of the
 glucopyranose unit (θ), and the vibrational correction (ζ). The
 angles φ and θ were calculated from positioning angles α and
 β . The latter pairs of angles were used in the course of numerical
 calculations, but they are not listed here. Their values are not
 important for the reader since they cannot be interpreted without
 the knowledge of the initial orientation of the rotated glucopy-
 ranose unit in the RDT coordinate frame.

First, let us notice that the analyzed relaxation data are
 reproduced well by the model of symmetric top. The highest
 departure of the best fit value from the experimental one of about
 15% has been obtained for cross-relaxation at the highest field
 exploited, i.e., 11.7 T. This happens since at higher magnetic
 fields the cross-relaxation rates are smaller compared to those
 at lower fields, so that the relative error of the measurement is
 larger. In other cases the discrepancies are about 4–5%.
 Inspection of Table 1 and Figure 2 reveals that the motional
 behavior of CDs does not change smoothly along with the
 number of glucopyranose units, n , in the CD cycle. **1** and **2**
 seem to depart significantly from the trend exhibited by the
 higher analogues. NMR data of the former molecules are better

T1

F2-3

352

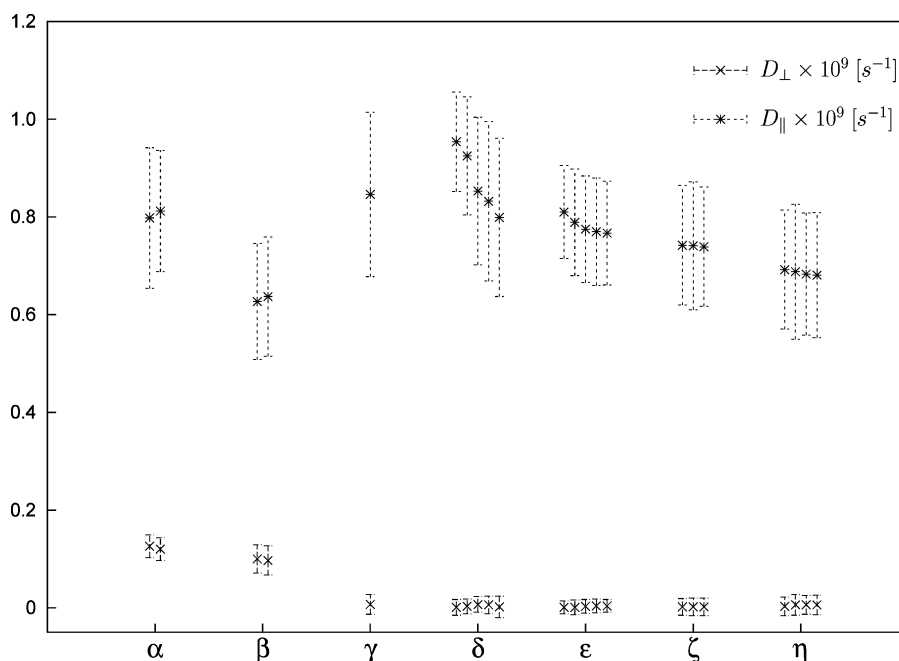


Figure 2. D_{\perp} and D_{\parallel} components of RDTs for cyclodextrins 1–7. The data are taken from columns 3 and 4 of Table 1. Error bars correspond to standard deviations.

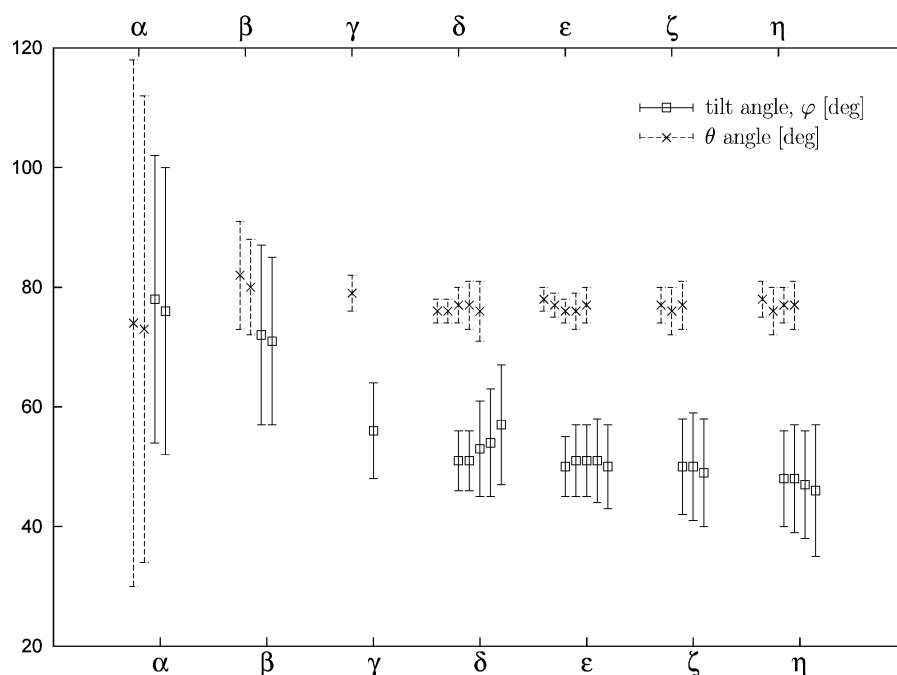


Figure 3. Angles θ and φ for cyclodextrins 1–7. The data are taken from columns 5 and 6 of Table 1. Error bars correspond to standard deviations. For the sake of clarity the upper x axis (θ angle) is slightly shifted with respect to the lower one (φ angle).

reproduced by the model of fast local dynamics, while for the latter ones the model of slow local motion works better. The GHW parameter is considerably lower for **1** and **2** than for the other CDs. This means that they tumble as rotors having a specific geometry while the geometries of larger CDs are “diffused” on the time scale of molecular tumbling. This is consistent with the intuitive belief that the ring-closing condition is much more restrictive for small CDs, so that their internal movement is more constrained than that of the larger ones. The magnitudes of the φ angle are consistent with this picture too. The molecular geometry becomes more diffused, and the averaged tilt angle of the glucopyranose unit relative to the xy plane of the respective RDT becomes smaller for larger CDs.

It is noteworthy that in all CDs the θ angle departs from 90° . Thus, in agreement with the CDs’ nonrigidity discussed in the Introduction, the glycosidic oxygen atoms are on average not coplanar. This statement is somewhat weakened by significant standard errors for the θ angle in **1** and **2**, but seems to be unquestionable for the remaining cycles. The mentioned large errors might stem from the possibility that the condition of fast local dynamics may not be strictly fulfilled for smaller CDs. Under such circumstances, the local dynamics would be a source of “extraneous” relaxation processes, which were not taken into account in the course of our analysis. For this reason we consider our results to be semiquantitative. This undescribed relaxation mechanism, together with neglected CSA relaxation, is a

TABLE 2: Comparison of the Determined Tilt Angles, φ , and Amplitudes of Glucopyranose Wagging, GHW, with Literature Data

	ref 48	ref 49 ^a	this paper
Tilt Angle (φ) (deg)			
α -CD	13 \pm 12	13 \pm 10	13 \pm 24
β -CD	13 \pm 13	14 \pm 10	18.5 \pm 15
γ -CD	9 \pm 17	19 \pm 9	34 \pm 8
Wagging Amplitude (GHW) (deg)			
α -CD	24 ^b		20–25
β -CD	38 ^b		25–30
γ -CD	50 ^b		55

^a Data obtained in the solid state by the X-ray diffraction method.

^b Determined approximately from Figure 7b of ref 48.

379 possible reason for slightly higher vibrational correction than
380 could be expected for CH bonds. Inspection of the last column
381 of Table 1 reveals that ζ never falls below 0.95 while the values
382 of 0.91–0.93 would be more plausible.

383 Finally, the determined parameters were used to reproduce
384 the $R_{1\rho C}$ data. Experimental and calculated values can be found
385 in the Supporting information. The agreement is very good for
386 **1** and **2**, while for the other CDs the applied model clearly fails.
387 One reason for this failure has already been mentioned above;
388 in CDs **3–7**, where the local dynamic is slower than the overall
389 molecular tumbling, the accurate calculations would require
390 unknown ^{13}C chemical shifts in individual conformers. Inspec-
391 tion of eqs 1–3 reveals, however, another possible reason for
392 the discrepancies. $R_{1\rho C}$ is the unique analyzed relaxation rate
393 which depends on the spectral densities at the ω_1 frequency,
394 which is at least 5 orders of magnitude smaller than ω_H and
395 ω_C . In CDs **3–7** the D_{\parallel} is 2 orders of magnitudes larger than
396 D_{\perp} . The latter is also much smaller than the Larmor frequencies
397 involved. This renders R_{1C} and ρ_C insensitive to the exact value
398 of D_{\perp} , which is then diminished in the course of the iterative
399 fitting process and delivered by the numerical routine with a
400 large standard error. D_{\perp} is, however, in the range where its
401 magnitude has a significant impact on spectral densities taken
402 at frequencies in the vicinity of ω_1 , i.e., on $R_{1\rho C}$. This seems to
403 be the main reason for the substantial discrepancies in the
404 reproduction of $R_{1\rho C}$ values for CDs **3–7**.

405 Finally let us remark that the relaxation behavior of the nuclei
406 within the methylene groups must be additionally influenced
407 by rotation about the C5–C6 bond. The latter process does not
408 appear to interfere much with the local dynamics considered
409 above. Accordingly, the relaxation data for the nuclei in these
410 side chains were not included in the analysis to avoid needless
411 complications of the problem addressed presently.

412 4. Conclusions

413 The nuclear spin relaxation data for CDs built of 6–12
414 glucopyranose units were investigated. The numerical iterative
415 analysis performed under the assumption of axially symmetric
416 RDTs described reasonably the results obtained. The RDT
417 components were determined along with the angles character-
418 izing the spatial arrangement of glucopyranose units in the RDT
419 coordinate frame. The components of RDTs do not change
420 smoothly with the CD size. D_{\perp} of **1** and **2** does not fit the trend
421 formed by larger CDs. The same seems to be true for D_{\parallel} , but
422 due to substantial errors which bear its values this statement is
423 somewhat weakened in the case of **1**. As expected,^{2,3} none of
424 the CDs occur in liquids as a rigid truncated-cone structure.
425 The internal motion in **1** and **2** seems to be faster than the overall

molecular tumbling, while for larger CDs the opposite is true. 426
The present observations seem to be consistent with the results 427
of molecular dynamics (MD) calculations by Naidoo et al.,^{47,48} 428
who concluded in ref 47 that **2** “undergoes small amplitude fast 429
librations” and “has a tendency to highly increase the local water 430
structure in the cavity and around the molecule” much more 431
than **1** and **3**. The values of the φ angle (which is equal to 90° 432
– θ in Naidoo’s notation) and GHW parameters extracted from 433
Figure 7b of ref 48 (see Table 2) also agree well with the present 434
results. 435

Acknowledgment. Financial support from the scientific 436
network “New applications of the nuclear magnetic resonance 437
spectroscopy in chemistry, biology, pharmacy and medicine” 438
is gratefully acknowledged. 439

Supporting Information Available: Experimental and 440
calculated values of NMR relaxation parameters and the 441
assignments of ^1H and ^{13}C NMR signals. This information is 442
available free of charge via the Internet at <http://pubs.acs.org>. 443

References and Notes 444

- (1) Dodziuk, H. In *Cyclodextrins and Their Complexes. Chemistry, Analytical Methods, Applications*; Dodziuk, H., Ed.; Wiley-VCH: Weinheim, Germany, 2006. 445
- (2) Dodziuk, H. *J. Mol. Struct.* **2002**, *614*, 33. 446
- (3) Dodziuk, H. In ref 1, Chapter 1.3. 447
- (4) Harata, K. In ref 1, Chapter 7.2. 448
- (5) Harata, K. In *Comprehensive Supramolecular Chemistry*; Szejtli, J., Ed.; Pergamon: Oxford, U.K., 1993; Vol. 3, Chapter 9. 449
- (6) Eliel, E. L.; Allinger, N. L.; Angyal, S. J.; Morrison, G. A. *Conformational Analysis*; Interscience: New York, 1965. 450
- (7) Dodziuk, H. In ref 1, Chapter 11. 451
- (8) Ejchart, A.; Kołmiński, W. In ref 1, Chapter 9. 452
- (9) Steiner, T.; Moreira, A. M.; Teixeira-Dais, J. J. C.; Müller, J.; Saenger, W. *Angew. Chem., Int. Ed.* **1995**, *34*, 1452. 453
- (10) Jullien, J.; Cacenill, J.; Lacombe, L.; Lehn, J.-M. *J. Chem. Soc., Perkin Trans. 2* **1994**, 989. 454
- (11) Ellwood, P.; Spencer, C. M.; Spencer, N.; Stoddart, J. F.; Zarzycki, R. *J. Inclusion Phenom. Mol. Recognit. Chem.* **1992**, *12*, 121. 455
- (12) Kowalewski, J.; Widmalm, G. *J. Phys. Chem.* **1994**, *98*, 28. 456
- (13) Ghalebani, L.; Kotsyubynskyy, D.; Kowalewski, J. *J. Magn. Reson.* **2008**, *195*, 1. 457
- (14) (a) Lipari, G.; Szabo, A. *J. Am. Chem. Soc.* **1982**, *104*, 4546. (b) Lipari, G.; Szabo, A. *J. Am. Chem. Soc.* **1982**, *104*, 4559. 458
- (15) Kowalewski, J.; Mäler, L. *Nuclear Spin Relaxation in Liquids: Theory, Experiments, and Applications*; Taylor and Francis: New York, 2006; Chapter 3. 459
- (16) (a) Endo, T.; Ueda, H.; Kobayashi, S.; Nagai, T. *Carbohydr. Res.* **1995**, *269*, 369. (b) Endo, T.; Nagase, H.; Ueda, H.; Kobayashi, S.; Nagai, T. *Chem. Pharm. Bull.* **1997**, *45*, 532. (c) Miyazawa, I.; Ueda, H.; Nagase, H.; Endo, T.; Kobayashi, S.; Nagai, T. *Eur. J. Pharm. Sci.* **1995**, *3*, 153. 460
- (17) Wishart, D. S.; Bigam, C. G.; Yao, J.; Abildgaard, F.; Dyson, H. J.; Oldfield, E.; Markley, J. L.; Sykes, B. D. *J. Biomol. NMR* **1995**, *6*, 135. 461
- (18) Farrow, N. E.; Muhandam, J. R.; Singer, A. U.; Pascal, S. M.; Kay, C. M.; Gish, G.; Shoelson, S. E.; Pawson, T.; Forman-Kay, J. D.; Kay, L. E. *Biochemistry* **1994**, *33*, 5984. 462
- (19) Dayie, K. T.; Wagner, G. *J. Magn. Reson., A* **1994**, *111*, 121. 463
- (20) Kay, L. E.; Nicholson, L. K.; Delaglio, F.; Bax, A.; Torchia, D. A. *J. Magn. Reson.* **1992**, *97*, 359. 464
- (21) Canet, D. *J. Magn. Reson.* **1976**, *23*, 361. 465
- (22) Delaglio, F.; Grzesiek, S.; Vuister, G. W.; Zhu, G.; Pfeifer, J.; Bax, A. *J. Biomol. NMR* **1995**, *6*, 277. 466
- (23) Goddard, T. D.; Kneller, D. G. *SPARKY 3*; University of California: San Francisco. 467
- (24) Fushman, D. In *BioNMR in Drug Research*; Zerbe, O., Ed.; Wiley-VCH: Weinheim, Germany, 2003; p 283. 468
- (25) Van Geet, A. L. *Anal. Chem.* **1968**, *40*, 2227. 469
- (26) Loening, N. M.; Keeler, J. *J. Magn. Reson.* **2002**, *159*, 55. 470
- (27) Press, W. H.; Teukolsky, S. A.; Vetterling, W. T.; Flannery, B. P. *Numerical Recipes: The Art of Scientific Computing*; Cambridge University Press: New York, 2007; Chapter 9. 471
- (28) Bernatowicz, P.; Kowalewski, J.; Szymański, S. *J. Chem. Phys.* **2006**, *124*, 024108. 472
- (29) Tropp, J. *J. Chem. Phys.* **1980**, *72*, 6035. 473
- (30) Korzhnev, D. M.; Bileter, M.; Arsenie, A. S.; Orekhov, V. Y. *Prog. NMR Spectrosc.* **2001**, *38*, 197. 474

Internal Dynamics in Cyclodextrins

- 500 (31) Luginbühl, P.; Wüthrich, K. *Prog. NMR Spectrosc.* **2002**, *40*, 199.
501 (32) Palmer, A. G., III. *Chem. Rev.* **2004**, *104*, 3623.
502 (33) Kempf, J. G.; Loria, J. P. *Cell Biochem. Biophys.* **2003**, *37*,
503 187.
504 (34) Chen, Y. Y.; Luo, S. Y.; Hung, S. C.; Chan, S. I.; Tzou, D. L. M.
505 *Carbohydr. Res.* **2005**, *340*, 723.
506 (35) Czugler, M.; Geiger, G.; Stezowski, J. J. Z. *Kristallogr.* **1983**, *162*,
507 54.
508 (36) Zabel, V.; Saenger, W.; Mason, S. A. *J. Am. Chem. Soc.* **1986**,
509 *108*, 3664.
510 (37) Saenger, W. *Nature (London)* **1979**, *279*, 343.
511 (38) Imamura, K.; Nimz, O.; Jacob, J.; Myles, D.; Mason, S. A.;
512 Kitamura, S.; Aree, T.; Saenger, W. *Acta Crystallogr., B* **2001**, *57*, 833.
513 (39) Le Bas, G.; Mason, S. A. *Acta Crystallogr., B* **1994**, *50*, 717.
514 (40) Steiner, T.; Mason, S. A.; Saenger, W. *J. Am. Chem. Soc.* **1990**,
515 *112*, 6184.
- (41) Steiner, T.; Mason, S. A.; Saenger, W. *J. Am. Chem. Soc.* **1991**, 516
113, 5676. 517
(42) Henry, E. R.; Szabo, A. *J. Chem. Phys.* **1985**, *82*, 4753. 518
(43) Case, D. A. *J. Biomol. NMR* **1999**, *15*, 95. 519
(44) Ottiger, M.; Bax, A. *J. Am. Chem. Soc.* **1998**, *120*, 12334. 520
(45) Kowalewski, J.; Effemey, M.; Jokisaari, J. *J. Magn. Reson.* **2002**, 521
157, 171. 522
(46) Bernatowicz, P.; Kowalewski, J.; Sandström, D. *J. Phys. Chem. A* 523
2005, *109*, 57. 524
(47) Naidoo, K. J.; Chen, J. Y.; Jansson, J. L. M.; Widmalm, G.; 525
Maliniak, A. *J. Phys. Chem. B* **2004**, *108*, 4236. 526
(48) Naidoo, K. J.; Gamielien, M. R.; Chen, J. Y.; Widmalm, G.; 527
Maliniak, A. *J. Phys. Chem. B* **2008**, *112*, 15151. 528
(49) Harata, K. *Chem. Rev.* **1998**, *98*, 1803. 529
- JP9084734 530